Received: 23 September 2023 | Revised: 10 November 2023 | Accepted: 17 November 2023

DOI: 10.1002/VIW.20230090

RESEARCH ARTICLE

The PES1/FOXM1 heterodimer suppresses TCF21 and ERβ expression in ovarian endometriosis

Jingwen Zhu | **Peili Wu** | **Ruihui Lu** | **Cheng Zeng** | **Chao Peng** | **Yingfang Zhou** | **Qing Xue**

Department of Obstetrics and Gynecology, Peking University First Hospital, Beijing, China

Correspondence
Qing Xue, Department of Obstetrics and Gynecology, Peking University First Hospital, No. 1 Xi'anmen Street, Beijing 100034, China.
Email: drxueqing@163.com

Funding information
Natural Science Foundation of Beijing, China, Grant/Award Number: 7202207

Abstract

Transcription factor 21 (TCF21) and estrogen receptor beta (ERβ, encoded by ESR2) are highly expressed in endometriotic stromal cells (ESCs) and contribute to the pathogenesis of endometriosis. However, the exploration of TCF21 and ERβ expression regulation at the molecular level remains limited. Here, by using bioinformatics analysis and experimental verification, we identified PES1, also known as Pescadillo, as a negative regulator in the development of endometriosis that downregulates TCF21 and ERβ expression in ESCs. PES1 overexpression regulated critical biological processes involved in endometriosis development, such as invasion and apoptosis. A coimmunoprecipitation assay showed that PES1 could form a complex with Forkhead box M1 (FOXM1). Further analyses elucidated that siPES1 in ectopic lesions decreased the stability of FOXM1 protein and reduced the binding activities of FOXM1 to TCF21 and ESR2 promoters, thus weakening the transcriptional inhibition of TCF21 and ERβ by FOXM1. Moreover, in an endometriosis mouse model, overexpressing PES1 effectively reduced the growth of ectopic lesions and suppressed TCF21 and ERβ expression, which suggests a promising therapeutic strategy for endometriosis. Collectively, our results indicate that the loss of PES1 in ectopic lesions contributes to endometriosis progression by upregulating ERβ and TCF21 expression through heterodimer formation with FOXM1. Moreover, targeting PES1 could serve as a treatment method for endometriosis.

KEYWORDS
adenovirus, endometriosis, estrogen pathway, pescadillo

1 | INTRODUCTION

Endometriosis is a chronic gynecologic disease in which the endometrial (EM)-like tissue is found outside the uterus. Approximately 10% of women experience this condition during their reproductive years.[1] The etiology of endometriosis is multifactorial, involving retrograde menstruation, hormonal imbalance, coelomic metaplasia, abnormal immune and inflammatory regulation, and epigenetic changes. Despite extensive research, the true

pathogenesis of endometriosis remains elusive.[2] Current treatments for endometriosis include surgical and medical therapies. However, considering the unfavorable side effects of hormonal therapy[3] and the high recurrence rate following surgery,[4] it is necessary to explore the core molecular targets in endometriosis to precisely treat this condition.

Exploration of the etiology of endometriosis has produced the consensus that endometriosis is an estrogen-dependent disorder. EM tissue growth is dominated by nuclear estrogen receptors (ERs) activated by biologically active estradiol.[5] ERβ (encoded by ESR2) and ERα (encoded by ESR1), are nuclear ER subtypes. The protein ratio of ERβ:ERα shows a visible increase in endometriotic stromal cells (ESCs) compared with eutopic EM cells.[6] Elevated ERβ levels can stimulate proinflammatory signaling, hypoxia signaling, and epithelial–mesenchymal transition and prevent apoptosis to promote ectopic lesion survival.[7] Meanwhile, we observed that transcription factor 21 (TCF21) is a critical upstream factor in the estrogen pathway. TCF21 can upregulate the expression of ERβ and steroidogenic factor 1 (SF-1), a core factor in estrogen synthesis, suggesting that TCF21 plays a pivotal role in the progression of endometriosis.[8] Nevertheless, our understanding of the mechanism by which ERβ is upregulated is deficient, and the relationship between TCF21 and ERβ coregulation is not yet known.

PES1, also known as Pescadillo or NOP7, plays a crucial role in embryonic development, cell cycle progression, DNA replication, chromosomal stability, and ribosome biogenesis.[9] PES1 is a multifunctional protein that can regulate HO-1 promoter activity in renal epithelial cells, implying its involvement in transcriptional regulation.[10] PES1 also contains a BRCA1 C-terminal (BRCT) domain, a structural motif that has been shown to promote protein–protein interactions.[11] Several studies have demonstrated that PES1 is upregulated in different types of tumors and has a significant role in tumor growth and progression.[12] PES1 can increase ERα levels and decrease ERβ levels, promoting breast and ovarian cancer development and progression by enhancing ERα stability and targeting ERβ for proteasomal degradation.[13] The above studies suggest a negative regulatory relationship between PES1 and ERβ. Until now, comprehensive studies regarding the functional roles of PES1 in endometriosis have been lacking.

Forkhead box M1 (FOXM1), belonging to the Forkhead transcription factor family, plays a pivotal role in the development of various cancers.[14] FOXM1 regulates cell-specific gene expression by binding DNA sites with the consensus sequence 5′-A-C/T-AAA-C/T-AA-3′.[15] A previous study showed that FOXM1 knockdown in human malignant pleural mesothelioma cell lines upregulated ERβ expression, but the exact mechanism is still unclear.[16] A few studies have suggested that FOXM1 is involved in the development of endometriosis.[17] Further investigation is required to determine the role of FOXM1 in endometriosis and its underlying mechanism.

Our investigation aimed to uncover the intricate molecular and cellular mechanisms by which PES1 regulates endometriosis progression. Herein, we observed that the expression levels of PES1 were significantly reduced in ESCs. Then, we demonstrated that PES1 forms heterodimers with FOXM1 to bind Forkhead response element (FHRE) sequences in the TCF21 and ESR2 gene promoters, ultimately reducing TCF21 and ESR2 expression in vitro. More importantly, based on our results in a mouse model, we speculate that targeting PES1 represents a promising therapeutic alternative for endometriosis.

2 | MATERIALS AND METHODS

2.1 | Participants

The study recruited female participants aged 25–40 years with a regular menstrual cycle who were surgically identified by laparoscopy as endometriosis. The study excluded women who received hormonal treatment for at least 3 months prior to surgery, those diagnosed with pelvic cysts, or those with other endocrine or metabolic diseases. Then, 15 self-controlled pairs of both eutopic EM tissues and ectopic EM tissues from the cyst walls of ovarian endometriomas (OMA) were collected from women who underwent laparoscopic excision of ovarian endometriosis with hysterectomy. The basic characteristics are summarized in Table 1. This study was carried out in compliance with the ethical guidelines set forth in the Declaration of Helsinki II and was granted approval by the Institutional Review Board of Peking University under reference number 2021[519]. Prior to the use of their samples, each patient provided written informed consent.

2.2 | Primary cell culture

The isolation of EM stromal cells and ESCs was carried out using a protocol modified from Ryan et al.[18] In brief, before chopping EM and OMA into small pieces, they were cleaned using sterile phosphate-buffered saline (PBS). Afterwards, the tissues were enzymatically digested for 1 h at 37°C using DNase (Sigma) and collagenase (1 mg/mL; Sigma). Following dissociation, the tissues

TABLE 1 Clinical characteristics of females with ovarian endometriosis.

Variable	Total ($n = 15$)	r-ASRM stage		*p*-Value
		Stage III ($n = 8$)	Stage IV ($n = 7$)	
Age (year)	35.53 ± 1.16	35.63 ± 1.44	35.43 ± 2.00	.800
BMI (kg/m^2)	21.81 ± 0.72	22.63 ± 1.23	20.88 ± 0.52	.613
CA125 level (U/mL)	49.37 ± 7.33	47.81 ± 6.20	51.16 ±14.72	.613
Menstrual average cycle (day)	28.00 ± 0.49	28.25 ± 0.75	27.71 ± 0.64	.476
Menstrual duration (day)	6.67 ± 0.27	6.25 ± 0.41	7.14 ± 0.26	.138
Menstrual cycle phase				.608
Proliferative phase	9/15	4/8	5/7	
Secretory phase	6/15	4/8	2/7	
Laterality of the cyst				.147
Left	6/15	4/8	2/7	
Right	6/15	4/8	2/7	
Bilateral	3/15	0/8	3/7	
Size of the cyst (mm)	64.53 ± 4.52	65.13 ± 6.60	63.86 ± 6.62	.933

Note: Statistical analysis was performed using Student's *t* test and Fisher's exact test. Data are mean ± SEM.

Abbreviations: BMI, body mass index; r-ASRM, revised American Society for Reproductive Medicine classification.

underwent two rounds of filtration before being resuspended in DMEM/F12 (1:1) (Gibco) added with fetal bovine serum (FBS; 10%, Gibco) and 1% Pen-Strep (M&C Gene Biotechnology). Experiments were performed before the fourth passage.

2.3 | Cell lines

The human EM cancer cell line ECC-1 was provided as a gift from Professor Jing Liang (Peking University Health Science Center). ECC-1 cells were cultured in RPMI-1640 medium (Gibco) supplemented with 10% FBS (Invitrogen) and 1% Pen-Strep. The incubation process was carried out in a humidified atmosphere, which contained 5% CO_2 and was maintained at 37°C.

2.4 | Next-generation RNA sequencing

RNA sequencing (RNA-seq) of four randomly selected paired EM and OMA tissues was performed using the Illumina HiSeq 2000/2500 platform, which generated 50-bp single-end reads. After obtaining the raw data in fastq format, we processed the data with custom Perl and Python scripts. To guarantee the accuracy and purity of our data, we undertook an essential measure that involved eliminating reads that exhibited poly-N sequences or 5′ adapter impurities and reds that lacked a 3′ adapter or insert tag. We also removed reads containing poly-A/T/G/C and low-quality reads, while calculating the raw data's Q20, Q30, and GC content. Finally, we carefully selected a precise range of refined reads for further analysis. Novogene Bioinformatics Technology (Beijing) conducted the sequencing and data collection.

2.5 | RNA extraction and quantitative analysis by real-time quantitative polymerase chain reaction

Total RNA was extracted from tissues and stromal cells using TRIzol (Invitrogen). In brief, we utilized 1 μg of RNA and the High-Capacity cDNA Archive Kit (Applied Biosystems) to perform reverse transcription. To quantify the mRNA levels, we employed an ABI 7500 sequence detection system and the ABI Power SYBR Green gene expression system (Applied Biosystems). Our internal control for this experiment was human GAPDH mRNA. The comparative threshold cycle method was used for relative quantification of all transcripts, as previously described.[19] The forward and reverse primers for PES1 were 5′- TCAACAAGTTCCGTGAATACAAG-3′ and 5′-GATGTGGTCGAGTTTGTAGTTG-3′; ESR2 primers were forward: 5′-ATGATCAGCTGGGCCAAGAA-3′ and reverse: 5′-CCACATCAGCCCCATCATTAA-3′; TCF21 primers were forward: 5′-AGCTACATCGCCCACTTGAG-3′ and reverse 5′-CGGTCACCACTTCTTTCAGG-3′; FOX M1 primers were forward: 5′-GGAGCAGCGACAGGTTAAG-3′ and reverse 5′-CCATGATACAATTCGCCATC AAC-3′; GAPDH primers were forward: 5′-GAAGG TGAAGGTCGGAGTC-3′ and 5′-GAAGATGGTGATGGGATTTC-3′.

2.6 | Western blotting

ESCs were lysed in RIPA buffer (Solarbio) supplemented with 1% protease inhibitor (Solarbio), and the protein concentrations were measured by a Bicinchoninic Acid (BCA) protein concentration assay kit (Solarbio). Sodium dodecyl sulfate polyacrylamide gel electrophoresis (SDS-PAGE) was used to separate equal amounts of protein on a 10% gel, which was then electroblotted onto polyvinylidene fluoride membranes (Millipore). The membranes were blocked with 5% nonfat dry milk (Sangon Biotech) for 1 h, after which they were subjected to incubation with primary antibodies overnight at 4°C. PES1 antibody (ab72539, 1:1000) and TCF21 antibody (ab182134, 1:1000) were purchased from Abcam. ERβ antibody (04842, 1:1000) was obtained from Merck Millipore. Anti-FOXM1 (D3F2B, 20459, 1:1000) was purchased from Cell Signaling Technology. Anti-GAPDH (TA-08, 1:1000) was purchased from ZSGB-BIO. After being washed five times in Tris-buffered Saline and Tween (TBST), the membranes were incubated with secondary antibody at 37°C for 1 h. Enhanced chemiluminescence solution (Syngene) was used to visualize the protein bands. Analysis of Western blot band intensities were conducted with ImageJ software.

2.7 | Small interfering RNA transfection

After reaching 80% confluence, Lipofectamine RNAiMAX was used to transfect ESCs with 100 nmol/L siRNA targeting the human PES1 or FOXM1 gene or a negative control siRNA, in Opti-MEM reduced serum medium (Invitrogen). The experiment was carried out following the manufacturer's instructions. After 24 or 48 h of incubation, the cells were harvested for RNA or protein isolation.

2.8 | Plasmid transfection

Before transfection, the ESCs were cultured until they reached approximately 80% confluence. Lipofectamine 3000 transfection reagent (Invitrogen) was used for transfection. The transfected plasmids included empty pENTER plasmid, pENTER-PES1 plasmid, empty pcDNA3.1 plasmid, or pcDNA3.1-FOXM1 plasmid (Vigene Biosciences). The process was carried out in accordance with the manufacturer's instructions. After 24 or 48 h of incubation, the cells were harvested for RNA or protein isolation.

2.9 | Flow cytometry analysis

To measure apoptosis, an Annexin V-FITC Apoptosis Detection Kit (BD Biosciences) was used. After collection, the ESCs were rinsed with ice-cold PBS and binding buffer. They were then incubated with Annexin V-FITC in the dark for at least 15 min. Next, propidium iodide was added and incubated for 10 min at room temperature in the dark, and apoptosis was analyzed using flow cytometry.

2.10 | Matrigel invasion assays

Matrigel invasion assays were performed using 24-well Transwell chambers (8-μm pore size, 6.5-mm diameter, Corning) coated with a 1:8 dilution of Matrigel (Corning). Afterwards, 2×10^5 primary ESCs that had been transfected with siRNA or plasmid were added to the top chamber without serum, while the lower chamber contained DMEM/F12 with 20% FBS. The cells were then incubated for 48 h at 37°C. The cells were collected from the upper filter surface and Matrigel using a cotton swab. The inserts were fixed in paraformaldehyde for 30 min and stained with crystal violet. To observe and image the stained cells on the lower surface, an Olympus DP71 microscope from Tokyo-based Olympus was used. Each experiment involved quantifying five randomly selected fields.

2.11 | Coimmunoprecipitation assay

Proteins were extracted from ESCs using a non-denaturing buffer with protease inhibitors. After centrifugation, part of the obtained supernatant was used as input group, and the other part was used for immunoprecipitation. This involved using anti-PES1 antibody (1:100; Abcam; ab72539), anti-FOXM1 antibody (1:50; Cell Signaling Technology; 20459) or IgG and Protein A agarose (Roche) to immunoprecipitate an equal amount of protein ranging from 500 to 1000 μg. The mixture was incubated at 4°C overnight and collected by centrifugation the next day. Western blotting was used to analyze the immunoprecipitates. The experiments were conducted on ESCs isolated from three different patients.

2.12 | Drug treatment

After transfection with the indicated plasmids or siRNAs, ESCs were divided into two groups. Mg132, a specific proteasome inhibitor of the 26S proteasome was given as the treatment group, and dimethylsulfoxide (DMSO) was given as the control group. The culture time was 6 h. To conduct the protein half-life experiment, cycloheximide (CHX, 100 μg/mL; MCE), a translation inhibitor, was added for the specified time intervals.

2.13 | Chromatin immunoprecipitation assay

The chromatin immunoprecipitation (ChIP) assay was conducted as previously described.[20] The cells underwent cross-linking, lysis, and enzymatic digestion and immunocoprecipitation was initiated. To serve as a control, 10% of each chromatin solution was used as an input. ChIP was conducted overnight at 4°C with an FOXM1 primary antibody (1:100; Cell Signaling Technology; 20459) and IgG antibody. The protein/DNA complexes were then eluted, and the purified DNA was analyzed using quantitative polymerase chain reaction (qPCR). The forward and reverse primers for ESR2 promoter were: 5′-GGGAGACTCTGCCTTTCAACC-3′ and 5′-TCCATCTTTGGAGCCTGTCTTC-3′. The forward and reverse primers for TCF21 promoter were 5′-CTGCTGTGGGAAGAGTCCTT-3′ (forward) and 5′-TGAATTAGCGACCCCTCTTCC-3′.

2.14 | Luciferase assay

Expression vectors encoding pcDNA3.1-FOXM1, the pGL3-TCF21 promoter, the pGL3-ESR2 promoter, the pGL3-TCF21-delete mutation promoter, and the pGL3-ESR2-delete mutation promoter (Vigene Biosciences) were transfected into ECC-1 cell line. We used 2 μg of a firefly luciferase reporter construct containing either the TCF21 or ESR2 promoter. Renilla luciferase reporter plasmid was used as an internal control. After 48 h, we measured the luciferase activity and standardized the firefly luciferase activity to the Renilla luciferase activity. We repeated the experiments independently three times.

2.15 | Induction of endometriosis

Female C57BL/6J mice (8 weeks old) were obtained from the Animal Research Laboratory of Peking University First Hospital. Endometriosis was surgically induced in the mice under aseptic conditions under anesthesia. Beginning on day 1, intramuscular injection of β-estradiol (0.1 mg/kg, Sigma) was given every 2 days. On the second day, a single side of the uterus was taken out and chopped into pieces. Afterwards, the fragmented uterus was stitched onto the peritoneal wall where the blood vessels are abundant of the same mouse. Twelve days after tissue transplantation, the mice were randomly divided into three groups: the PBS group, the adenovirus vector group (1×10^9 plaque forming units [pfu]), and the Pes1 adenovirus group (1×10^9 pfu). They were then injected with either PBS or adenovirus (Vigene Biosciences) every 7 days. After 28 days, the mice were sacrificed. To calculate the volume of the ectopic lesions, we used the formula volume = 0.5 × length × width^2. We then harvested the implanted EM lesions for further analysis. Animal experiments were approved by the Peking University First Hospital Animal Care and Use Committee (J2023103).

2.16 | Statistical analysis

The data are shown as the mean ± SEM, with statistical analysis performed using SPSS 26.0 software. When comparing two groups, a two-tailed Student's t test was used, while comparisons among more than two groups were conducted using one-way analysis of variance. The results with a p value <.05 were considered statistically significant.

3 | RESULTS

3.1 | The expression of PES1 is downregulated in endometriosis

To investigate the candidate key endometriosis-related genes, paired EM and OMA tissues were subjected to RNA-seq screening. PES1 was found to be remarkably downregulated in OMA compared with EM tissue (Figure 1A). The findings of RNA-seq analysis and real-time (RT)-qPCR findings were consistent with each other, confirming a significant decrease in PES1 mRNA levels in the OMA tissue in comparison to the EM tissue (Figure 1B). Moreover, the Western blotting results demonstrated that PES1 protein expression was also significantly lower in the OMA (Figure 1C). Subsequently, human primary eutopic EMs and ESCs were isolated from the collected EM and endometriotic tissues. The expression levels of PES1 mRNA (Figure 1D) and protein (Figure 1E) were consistently decreased in ESCs compared with EMs.

3.2 | PES1 promotes the development of endometriosis by regulating crucial pathological processes

Previous studies have suggested that PES1 can affect the estrogen pathway,[12] and the hypoestrogenic environment is a critical pathological condition for endometriosis. Therefore, we asked whether PES1 could regulate TCF21, a key upstream factor of the estrogen pathway, and ERβ, the major ER subtype in endometriosis. To provide additional evidence for the roles of PES1 in the regulation of TCF21 and ERβ expression, we used siRNAs to knock down PES1

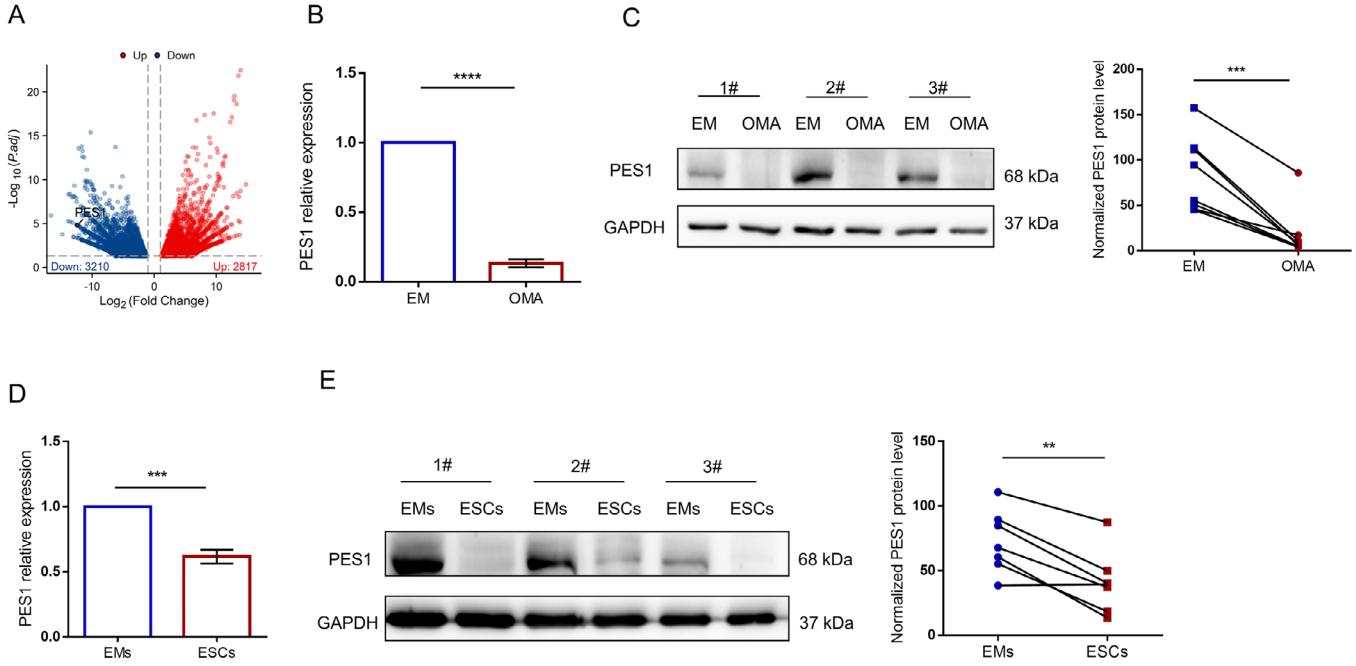

FIGURE 1 The expression of PES1 is downregulated in endometriosis. A, Volcano plots of differentially expressed genes between endometrial (EM) and ovarian endometriomas (OMA) tissues (Fold change > 2, $p < .05$). B, RNA was extracted from 15 pairs of EM and OMA, and PES1 mRNA levels were quantified using real-time quantitative polymerase chain reaction (RT-qPCR). C, PES1 protein level between EM and OMA tissues was compared by Western blotting ($n = 6$ subjects in each group; left panel). Normalization was done using GAPDH ($n = 6$ subjects in each group; right panel). D, Total RNA was extracted from seven paired EMs and endometriotic stromal cells (ESCs) isolated from paired eutopic and ectopic endometria. PES1 mRNA levels were measured using RT-qPCR ($n = 7$ subjects in each group). E, Western blotting was performed to compare the protein levels of PES1 between EMs and ESCs ($n = 7$ subjects in each group; left panel). The expression levels were quantified and normalized to GAPDH ($n = 7$ subjects in each group; right panel). The results of all experiments are expressed as the mean ± SEM of three independent experiments, and Student's *t* test was used for data analysis (**$p < .01$, ***$p < .001$, ****$p < .0001$).

and assessed the knockdown efficacy by both RT-qPCR and Western blotting (Figure 2A,B). We found that knockdown of PES1 resulted in a significant upregulation in the expression of TCF21 and ERβ (Figure 2A,B). In contrast, plasmid transfection was used to overexpress PES1 in ESCs (Figure 2C,D), and we found that overexpression of PES1 suppressed TCF21 and ERβ mRNA expression (Figure 2C) and protein levels (Figure 2D). Together, these results indicate that PES1 exerts an inhibitory effect on TCF21 and ERβ expression in ESCs. Given the abnormal PES1 expression in endometriosis and the known role of PES1 in regulating apoptosis and cell invasion,[21] we speculated that PES1 could possibly regulate the invasion and apoptosis of EM cells. To test this hypothesis, ESCs were transfected with PES1–siRNA or PES1 overexpression plasmid. Flow cytometry showed a higher percentage of apoptotic cells in ESCs overexpressing PES1 compared to control, while siPES1 transfection inhibited ESC apoptosis (Figure 2E). Transwell assays showed that ESC invasion was induced by PES1 downregulation and reduced by PES1 upregulation (Figure 2F). These data demonstrated that loss of PES1 expression resulted in enhanced invasion and decreased apoptosis of ESCs.

3.3 | PES1 forms a complex with FOXM1

Tandem affinity preparation/mass spectrometry analysis was performed to identify transcription factor interacting proteins in HEK293T cells, and the results showed that PES1 and FOXM1 could interact with each other.[22] To explore whether this interaction also exists in ectopic lesions, we first found and verified that FOXM1 mRNA expression was also downregulated in OMA (Figure 3A,B). Moreover, FOXM1 expression was downregulated in ESCs (Figure 3C,D). Then, we used the three-dimensional structure of FOXM1 and PES1 to predict the interaction between the two proteins and found that the confidence score for their combination was as high as 0.911 (Figure 3E). A coimmunoprecipitation assay was performed to confirm the complex formation between PES1 and FOXM1 in ESCs, as shown in Figure 3F. PES1 can affect the ubiquitination and degradation of proteins,[13a] so we wanted to explore whether PES1 could affect the protein stability of FOXM1. To test this hypothesis, we transfected ESCs with a control siRNA or siPES1 and found that PES1 knockdown resulted in a significant decrease in FOXM1 protein levels (Figure 3H) but not mRNA levels (Figure 3G). We

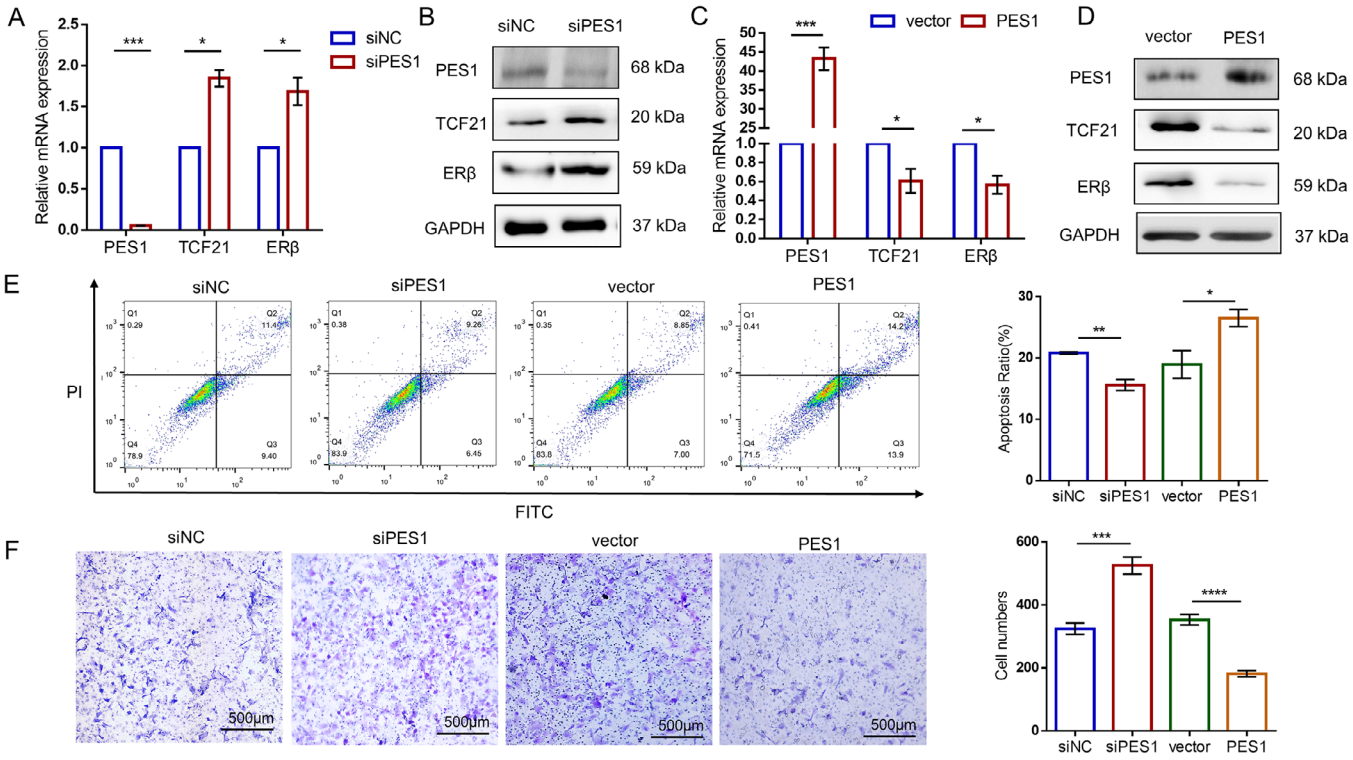

FIGURE 2 PES1 promotes the development of endometriosis via regulation of crucial processes. A and B, Endometriotic stromal cells (ESCs) were transfected with PES1 or control siRNA. The levels of PES1, transcription factor 21 (TCF21), and estrogen receptor beta (ERβ) were measured by real-time quantitative polymerase chain reaction (RT-qPCR) ($n = 5$) or Western blotting ($n = 3$). C and D, ESCs were transfected with PES1 overexpression or control plasmid. The levels of PES1, TCF21, and ERβ were measured by RT-qPCR ($n = 5$) or Western blotting ($n = 3$). E, Flow cytometry analysis was performed on ESCs transfected with expression plasmids and/or siRNAs to assess PES1's impact on apoptosis rate ($n = 3$). F, ESCs were transfected with siRNAs or plasmid and invasion was measured at 48 h using Matrigel invasion chambers ($n = 3$; scale bar, 500 μm). The results of all experiments are expressed as the mean ± SEM of three independent experiments, and Student's *t* test and one-way analysis of variance (ANOVA) were used for data analysis (*$p < .05$, **$p < .01$, ***$p < .001$, ****$p < .0001$).

subsequently found that administration of Mg132 reversed the decline in FOXM1 protein levels caused by PES1 knockdown (Figure 3I), suggesting that PES1 affects the stability of FOXM1. Moreover, CHX chase assays showed that PES1 knockdown was associated with an evident decrease in the half-life of FOXM1 (Figure 3J), indicating that PES1 maintains FOXM1 protein stability.

3.4 | Transcription repression of TCF21 and ERβ by the PES1–FOXM1 complex

FOXM1, as a transcription factor, recognizes and binds FHRE in target genes to control transcription.[15] Combining data from the University of California Santa Cruz and JASPAR databases, we found FHRE sequences in the gene promoter regions of both ESR2 and TCF21. To determine whether FOXM1 can regulate TCF21 and ERβ expression at the transcriptional level, we transfected FOXM1 siRNA and plasmids into ESCs. We found that the mRNA and protein levels of TCF21 and ERβ were increased (Figure 4A,C) by FOXM1 knockdown but decreased (Figure 4B,C) by FOXM1 overexpression. ChIP assays were conducted to confirm that FOXM1 has the ability to bind to the promoter regions of TCF21 and ESR2. Based on the results displayed in Figure 4D, the binding affinities between FOXM1 and the ESR2 and TCF21 promoters were significantly lower in ESCs than in EMs (Figure 4D). To identify the transcriptional regulatory components within the TCF21 and ESR2 promoters, we utilized a reporter construct with a deletion mutation specific to the binding site and transfected it into ECC-1 cells, after which promoter activity was assessed using luciferase assays. As shown in Figure 4E, FOXM1 was able to repress TCF21 and ESR2 promoter activity, but only when the FHRE sequence was present. TCF21 and ESR2 promoters lacking this sequence did not respond to FOXM1. We next investigated the functional importance of PES1 in the formation and chromatin targeting of the PES1–FOXM1 complex. ChIP assays revealed that the binding of FOXM1 to the TCF21 and ESR2 promoters was significantly reduced by knockdown of PES1 (Figure 4F). Moreover, FOXM1 was no longer able to repress

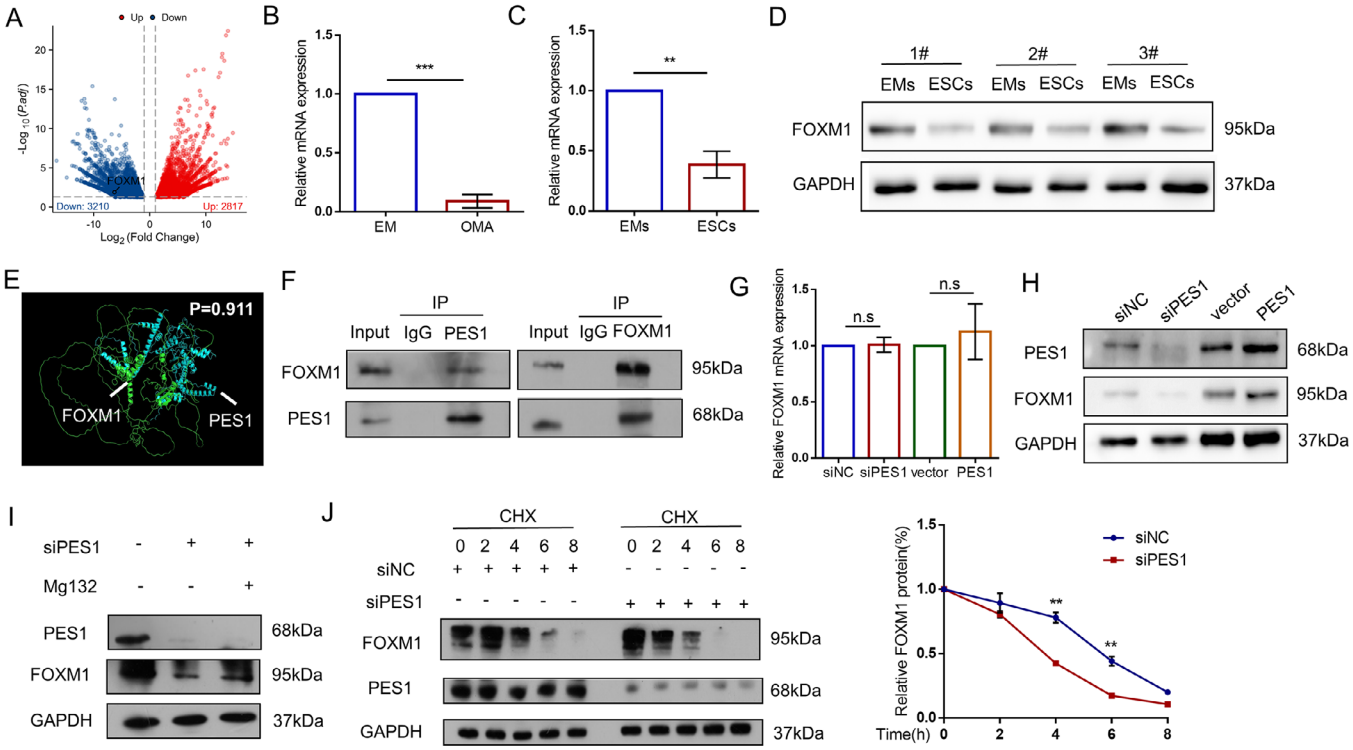

FIGURE 3 PES1 forms a complex with Forkhead box M1 (FOXM1). A, Volcano plots of differentially expressed genes between endometrial (EM) and ovarian endometriomas (OMA) tissues (Fold change > 2, $p < .05$). B, Total RNA was extracted from paired EM and OMA samples, and FOXM1 mRNA levels were quantified by real-time quantitative polymerase chain reaction (RT-qPCR) ($n = 6$). C, Total RNA was extracted from five paired EMs and endometriotic stromal cells (ESCs) isolated from paired eutopic and ectopic endometria. FOXM1 mRNA levels were measured using RT-qPCR. D, Western blotting was performed to compare the protein levels of FOXM1 between EMs and ESCs ($n = 6$). E, FOXM1 and PES1 3D structure interaction prediction model ($p = .911$). F, ESCs lysates were collected and immunoprecipitated with anti-PES1, anti-FOXM1, or anti-IgG antibody. The samples were analyzed by Western blotting with anti-FOXM1 and anti-PES1 antibody ($n = 3$; IP, immunoprecipitation). G and H, ESCs were transfected with the indicated expression constructs and/or siRNAs, and FOXM1 expression was measured by qPCR and Western blotting. I, ESCs were transfected with the indicated siRNA 18 h and were then treated without (control) or with 10 μM Mg132 for 6 h. FOXM1 protein levels were analyzed by Western blotting ($n = 3$). J, ESCs transfected with siPES1 and siNC were treated with 100 μg/mL cycloheximide (CHX) at the indicated time periods. The cell extracts were subjected to Western blot analysis. The levels of the remaining FOXM1 protein were normalized to those of GAPDH and plotted relative to the levels at the 0 h time point ($n = 3$). The results of all experiments are expressed as the mean ± SEM of three independent experiments, and Student's t test and one-way analysis of variance (ANOVA) were used for data analysis (**$p < .01$, ***$p < .001$).

TCF21-Luc or ESR2-Luc activity when PES1 was knocked down (Figure 4G), further supporting the targeting of the TCF21 and ESR2 genes by the PES1–FOXM1 complex.

3.5 | The therapeutic role of PES1 overexpression in endometriosis

To determine whether PES1 plays an important role in endometriosis development in vivo, we established a mouse model of endometriosis via uterine tissue autotransplantation. Eighteen mice were randomly divided into three groups: the PBS group, the empty adenovirus vector group (Ad-empty), and the Pes1 adenovirus group (Ad-Pes1). Endometriotic implants were stained with hematoxylin and eosin staining to confirm the presence of EM epithelial cell (black arrow) and stromal cell (white arrow) (Figure 5A). The protein levels of Pes1 in ectopic implants were confirmed to have been increased in the Ad-Pes1 group by immunohistochemistry (Figure 5B), indicating the successful upregulation of PES1 expression by Ad-PES1 injection. Then, we found that Pes1 overexpression significantly reduced the weight and volume of endometriotic-like lesions (Figure 5C). Furthermore, the Western blot analysis of the tissue grafts revealed a decrease in TCF21 and ERβ protein levels in the Ad-PES1 group compared to the Ad-empty and PBS groups (Figure 5D). These findings demonstrate that PES1 plays a crucial role in endometriosis development and that overexpressing PES1 may be a promising therapeutic approach.

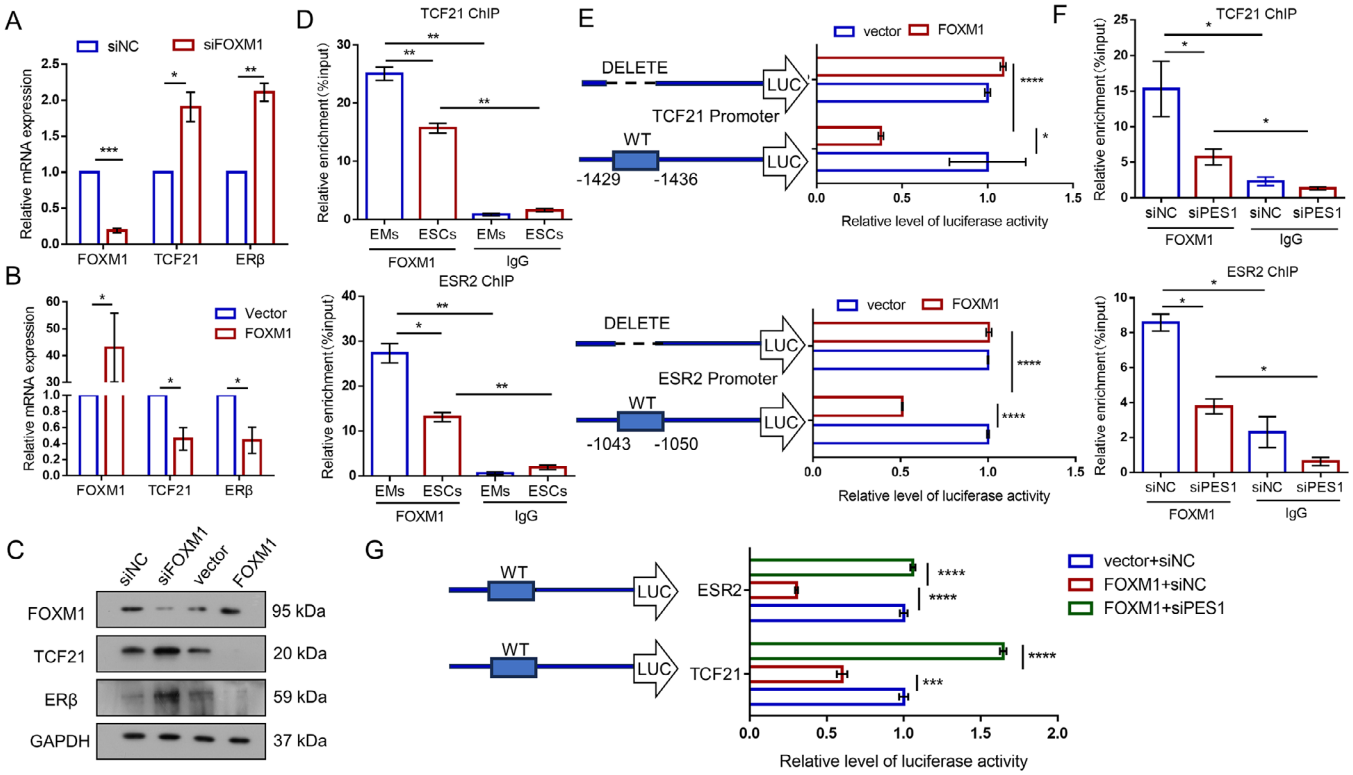

FIGURE 4 Transcription repression of transcription factor 21 (TCF21) and estrogen receptor beta (ERβ) by PES1–Forkhead box M1 (FOXM1) complex. A and C, Endometriotic stromal cells (ESCs) were transfected with FOXM1 or control siRNA, and FOXM1, TCF21, and ERβ expression was measured by quantitative polymerase chain reaction (qPCR) ($n = 3$) or Western blotting ($n = 3$). B and C, ESCs were transfected with a FOXM1 overexpression plasmid or vector, and FOXM1, TCF21, and ERβ expression was measured by qPCR ($n = 5$) or Western blotting ($n = 3$). D, Harvested paired eutopic and ectopic endometrial stromal cells underwent chromatin immunoprecipitation (ChIP) with anti-FOXM1 or control IgG antibody, followed by SYBR green-based qPCR ($n = 3$). E, Reporter plasmids containing the TCF21 or ESR2 promoter with either a wild-type sequence or delete sequence were transiently transfected into ECC-1 cells, and luciferase activity was measured ($n = 3$). F, ESCs were transfected with the control or PES1 siRNA. qChIP analysis of the TCF21 and ESR2 promoters was performed using antibodies against FOXM1 or IgG ($n = 3$). G, ECC-1 cells were transfected with control or PES1 siRNA, TCF21-Luc or ESR2-Luc, and FOXM1 expression constructs. Luciferase activity was measured after 48 h, and the relative activity was calculated and compared to the control ($n = 3$). The results of all experiments are expressed as the mean ± SEM of three independent experiments, and Student's *t* test and one-way analysis of variance (ANOVA) were used for data analysis (*$p < .05$, **$p < .01$, ***$p < .001$, ****$p < .0001$).

4 | DISCUSSION

To our knowledge, this study provides the first direct evidence of the biological and pathological role of PES1 in the development of ovarian endometriosis. In this study, we showed that PES1 expression levels were decreased in ectopic EM tissues and stromal cells. PES1 downregulated ERβ and TCF21 expression by enhancing the binding of the transcription factor FOXM1 to the ESR2 and TCF21 promoter regions, which further suppressed invasion activity and promoted apoptosis. More importantly, we demonstrated that by overexpressing PES1, the development of endometriotic lesions was prevented. Altogether, these results suggest that PES1 has therapeutic potential for endometriosis.

PES1 usually functions as an oncogene, promoting the development of multiple human cancers.[23] PES1 modulates the balance and ratio of the ERα and ERβ proteins, and this regulation is involved in the occurrence and development of breast, ovarian, and papillary thyroid cancers.[13,24] Mechanistically, PES1 enhances ERα stability and reduces ERβ stability via carboxyl terminus of Hsc70-interacting protein (CHIP)-mediated ubiquitin–proteasome pathway.[13a] Notably, this imbalance in the ERα and ERβ ratio is also present in ectopic lesions[6] and may be involved in the pathogenesis of endometriosis. Consistent with a previous study, our results demonstrated that PES1 has a negative regulatory effect on ERβ expression. The difference is that previous studies focused on the regulation of PES1 at the ERβ protein level without exploring its influence at the mRNA level. Our study found that PES1 can inhibit the expression of ERβ at the transcriptional level. In addition, PES1 inhibits transcriptional activity of ERβ, a tumor suppressor in breast cancers,

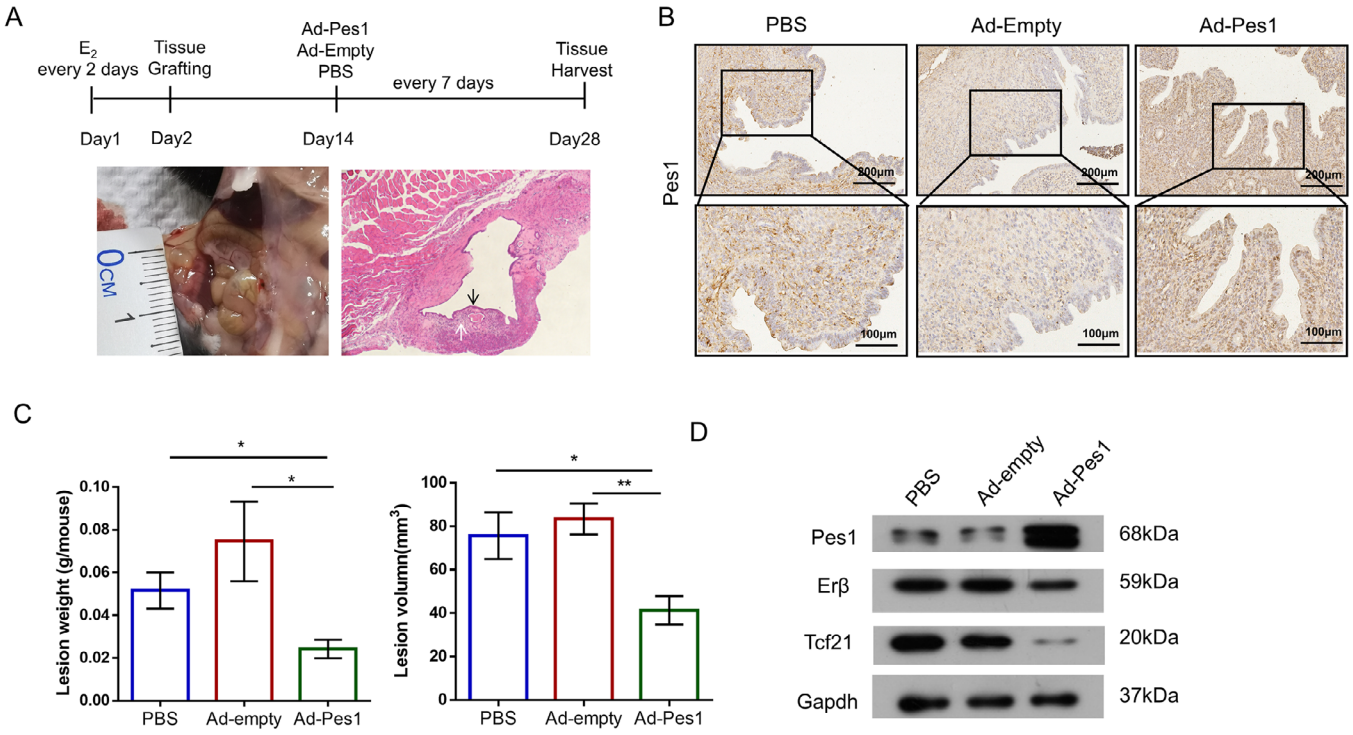

FIGURE 5 The therapeutic effect of PES1 overexpression in endometriosis. A, Mice were sacrificed, and their graft tissues underwent hematoxylin and eosin (H&E) staining to confirm endometriosis histological characteristics ($n = 6$ mice per group; scale bar, 100 μm). B, Immunohistochemistry (IHC) analyses of Pes1 levels in the ectopic lesions of PBS, Ad-empty, and Ad-Pes1 groups ($n = 3$ mice per group; scale bar, 100 μm, 200 μm). C, The volume and weight of established endometriotic lesions were assessed in indicated groups after induced endometriosis ($n = 6$ per group). D, Proteins were extracted from ectopic lesions from mice in the three groups, and Western blotting was performed.

and thus modulates many estrogen-responsive genes.[13a] However, in endometriotic tissue, a switch from ESR1 to ESR2 dominance occurs. Abnormally high levels of ESR2 regulate pathological processes in ectopic lesions, including invasion, proliferation, and apoptosis inhibition. This was previously discovered by researchers and our team.[25] These findings may explain why PES1 plays an oncogenic role in tumors but is a negative regulator in endometriosis. Additionally, there have been no reports that PES1 affects TCF21 expression prior to our present study. Thus, our study adds another pathological function of PES1 by demonstrating its critical roles in endometriosis.

PES1 can exert its regulatory role by forming complexes with other proteins. The PeBoW complex, consisting of PES1, BOP1, and WDR12, drives cell proliferation by facilitating the maturation of ribosomal RNA and subunits.[26] In addition, by directly interacting with TERT, PES1 plays a crucial role in regulating telomerase activity, maintaining telomere length, and controlling cellular senescence.[27] A previous analysis of purified HEK293T cells indicated an interaction between PES1 and FOXM1, but the mass spectrometry findings were not verified.[22] In this study, we provide evidence of the interactions between PES1 and FOXM1 in ESCs. Previous studies have found that PES1 can interact with the E3 ligase CHIP to affect protein ubiquitination. Our study also confirmed that PES1 can regulate protein stability; that is, PES1 stabilizes FOXM1 protein expression by affecting ubiquitination. However, the E3 ligase that affects FOXM1 ubiquitination still needs further investigation. In addition, a recent study found that the expression level of CHIP in ectopic lesions is decreased,[28] which is consistent with the trend in PES1 expression. Therefore, the relationship between PES1–CHIP complex-induced ubiquitination and the development of endometriosis is worth exploring.

FOXM1 is one of the most frequently overexpressed proteins in human solid cancers and has been implicated in promoting tumor proliferation, invasion, angiogenesis, drug resistance, cancer stem cell renewal, and cancer differentiation.[29] However, previous studies have also reported that endothelial-specific deletion of FOXM1 can increase the occurrence of urethane-induced lung cancer indicating FOXM1 has a tumor suppressive effect on lung endothelial cells,[30] suggesting that FOXM1 can play different roles in different disease environments. Our research found that FOXM1 levels decrease in endometriosis lesions, which restricts development by downregulating TCF21 and ERβ expression. However, Zhang et al. showed

that FOXM1 expression in the ectopic endometrium was higher compared to that in the paired eutopic EM tissues, suggesting that FOXM1 promotes the development of endometriosis.[17a] However, this study only used immunohistochemistry to determine differences in expression, which may have resulted in different results due to the limitations of the experimental methods. Moreover, a recent study used a cDNA-based expression array to explore gene expression differences between paired eutopic and ectopic endometria, and FOXM1 was found to be downregulated in ectopic lesions.[31] Our study, based on transcriptome sequencing, verified that at both mRNA and protein expression level, FOXM1 was significantly downregulated in ectopic lesions, which was consistent with the above finding.

Previous studies on FOXM1 have focused on its stimulatory activities in upregulating gene expression for tumor progression. However, FOXM1 also has a repressor function.[32] FOXM1-Rb complex downregulates luminal differentiation gene FOXA1, mammary differentiation gene Gata3, and tumor suppressor Pten in breast cancer cells.[32,33] The correlation between FOXM1 and the estradiol signaling pathway has been studied in breast cancer.[34] FOXM1 can activate the transcriptional activity of the ERα promoter via interaction with the coactivator CARM1. Previous studies have reported that knocking down FOXM1 in human malignant pleural mesothelioma cell lines leads to an increase in expression levels of ERβ,[16] but this study did not explore its molecular mechanism. Our study is the first to show that FOXM1 inhibits transcription by binding to the FHRE motif in the promoter region of TCF21 and ESR2 genes and that PES1 can enhance the transcriptional inhibition of FOXM1 by stabilizing its expression.

Altogether, our study suggests that the decreased expression level of PES1 in ectopic lesions reduces the stability of the FOXM1 protein, weakens the transcriptional inhibition of ERβ and TCF21 by FOXM1, and further promotes the development of endometriosis. Moreover, overexpression of PES1 resulted in the downregulation of TCF21 and ERβ expression, effectively halting the growth of ectopic lesions in mice. Cumulatively, the results indicate that PES1 plays a crucial role in endometriosis pathogenesis, making it a promising target for future therapy.

AUTHOR CONTRIBUTIONS

Jingwen Zhu performed the experiments. Jingwen Zhu and Peili Wu designed research. Ruihui Lu and Cheng Zeng performed the analysis with constructive discussions. Chao Peng and Yingfang Zhou performed the laparoscopic surgery. Qing Xue revised the manuscript.

ACKNOWLEDGMENTS

The authors would like to thank Professor Ding-Fang Bu for his valuable advice on this study. This study was funded by the Natural Science Foundation of Beijing, China (grant number 7202207).

CONFLICT OF INTEREST STATEMENT

The authors declare no conflict of interest.

DATA AVAILABILITY STATEMENT

The data are available from the corresponding author upon reasonable request.

ORCID

Qing Xue https://orcid.org/0000-0001-9608-8331

REFERENCES

1. A. W. Horne, S. A. Missmer, *BMJ* **2022**, *379*, e070750.
2. P. G. Signorile, R. Viceconte, A. Baldi, *Front. Med.* **2022**, *9*, 879015.
3. P. R. C. França, A. C. P. Lontra, P. D. Fernandes, *Molecules* **2022**, *27*, 4034.
4. S. W. Guo, *Hum. Reprod. Update* **2009**, *15*, 441.
5. E. Chantalat, M. C. Valera, C. Vaysse, E. Noirrit, M. Rusidze, A. Weyl, K. Vergriete, E. Buscail, P. Lluel, C. Fontaine, J. F. Arnal, F. Lenfant, *Int. J. Mol. Sci.* **2020**, *21*, 2815.
6. Q. Xue, Z. Lin, Y. H. Cheng, C. C. Huang, E. Marsh, P. Yin, M. P. Milad, E. Confino, S. Reierstad, J. Innes, S. E. Bulun, *Biol. Reprod.* **2007**, *77*, 681.
7. a) S. J. Han, S. Y. Jung, S. P. Wu, S. M. Hawkins, M. J. Park, S. Kyo, J. Qin, J. P. Lydon, S. Y. Tsai, M. J. Tsai, F. J. DeMayo, B. W. O'Malley, *Cell* **2015**, *163*, 960; b) S. J. Han, J. E. Lee, Y. J. Cho, M. J. Park, B. W. O'Malley, *Endocrinology* **2019**, *160*, 2495.
8. a) P. L. Wu, Y. Zhou, C. Zeng, X. Li, Z. T. Dong, Y. F. Zhou, S. E. Bulun, Q. Xue, *Biochim. Biophys. Acta. Gene Regulat. Mech.* **2018**, *1861*, 706; b) J. Zhu, P. Wu, C. Zeng, Q. Xue, *Biol. Reprod.* **2021**, *105*, 128.
9. a) M. L. Allende, A. Amsterdam, T. Becker, K. Kawakami, N. Gaiano, N. Hopkins, *Genes Dev.* **1996**, *10*, 3141; b) S. Gessert, D. Maurus, A. Rössner, M. Kühl, *Dev. Biol.* **2007**, *310*, 99; c) A. Lerch-Gaggl, J. Haque, J. Li, G. Ning, P. Traktman, S. A. Duncan, *J. Biol. Chem.* **2002**, *277*, 45347.
10. E. M. Sikorski, T. Uo, R. S. Morrison, A. Agarwal, *J. Biol. Chem.* **2006**, *281*, 24423.
11. M. Kellner, M. Rohrmoser, I. Forné, K. Voss, K. Burger, B. Mühl, A. Gruber-Eber, E. Kremmer, A. Imhof, D. Eick, *Exp. Cell Res.* **2015**, *334*, 146.
12. Y. Z. Li, C. Zhang, J. P. Pei, W. C. Zhang, C. D. Zhang, D. Q. Dai, *J. Cancer* **2022**, *13*, 268.
13. a) L. Cheng, J. Li, Y. Han, J. Lin, C. Niu, Z. Zhou, B. Yuan, K. Huang, J. Li, K. Jiang, H. Zhang, L. Ding, X. Xu, Q. Ye, *J. Clin. Investig.* **2012**, *122*, 2857; b) J. Li, Q. Zhuang, X. Lan, G. Zeng, X. Jiang, Z. Huang, *IUBMB Life* **2013**, *65*, 1017.
14. S. Borhani, A. L. Gartel, *Expert Opin. Therap. Targets* **2020**, *24*, 205.

15. D. R. Littler, M. Alvarez-Fernández, A. Stein, R. G. Hibbert, T. Heidebrecht, P. Aloy, R. H. Medema, A. Perrakis, *Nucleic Acids Res.* **2010**, *38*, 4527.
16. G. Pinton, S. Zonca, A. G. Manente, M. Cavaletto, E. Borroni, A. Daga, P. V. Jithesh, D. Fennell, S. Nilsson, L. Moro, *Oncotarget* **2016**, *7*, 14366.
17. a) J. Zhang, Z. Xu, H. Dai, J. Zhao, T. Liu, G. Zhang, *Gynecol. Obstetr. Investig.* **2019**, *84*, 485; b) P. Jin, X. Chen, G. Yu, Z. Li, Q. Zhang, J. V. Zhang, *Anti-Cancer Agents Med. Chem.* **2019**, *19*, 323.
18. I. P. Ryan, E. D. Schriock, R. N. Taylor, *J. Clin. Endocrinol. Metab.* **1994**, *78*, 642.
19. K. J. Livak, T. D. Schmittgen, *Methods* **2001**, *25*, 402.
20. J. N. Xu, C. Zeng, Y. Zhou, C. Peng, Y. F. Zhou, Q. Xue, *J. Clin. Endocrinol. Metab.* **2014**, *99*, 2795.
21. a) Z. Jiang, Y. Zhang, X. Chen, Y. Wang, P. Wu, C. Wu, D. Chen, *J. Transl. Med.* **2020**, *18*, 209; b) M. Nakaguro, S. Kiyonari, S. Kishida, D. Cao, Y. Murakami-Tonami, H. Ichikawa, I. Takeuchi, S. Nakamura, K. Kadomatsu, *Cancer Sci.* **2015**, *106*, 237; c) Y. He, J. Xiang, Y. Li, W. Huang, F. Gu, Y. Wang, R. Chen, *Cancer Med.* **2023**, *12*, 12622.
22. X. Li, W. Wang, J. Wang, A. Malovannaya, Y. Xi, W. Li, R. Guerra, D. H. Hawke, J. Qin, J. Chen, *Mol. Syst. Biol.* **2015**, *11*, 775.
23. a) X. Jin, R. Fang, P. Fan, L. Zeng, B. Zhang, X. Lu, T. Liu, *J. Exp. Clin. Cancer Res. CR* **2019**, *38*, 463; b) N. Ma, R. Hua, Y. Yang, Z. C. Liu, J. Pan, B. Y. Yu, Y. F. Sun, D. Xie, Y. Wang, Z. G. Li, *J. Biomed. Sci.* **2023**, *30*, 20; c) Z. Bian, M. Zhou, K. Cui, F. Yang, Y. Cao, S. Sun, B. Liu, L. Gong, J. Li, X. Wang, C. Li, S. Yao, Y. Yin, S. Huang, B. Fei, Z. Huang, *J. Exp. Clin. Cancer Res. CR* **2021**, *40*, 360.
24. Y. B. Qiu, L. Y. Liao, R. Jiang, M. Xu, L. W. Xu, G. G. Chen, Z. M. Liu, *Sci. Rep.* **2019**, *9*, 1032.
25. a) B. D. Yilmaz, S. E. Bulun, *Hum. Reprod. Update* **2019**, *25*, 473; b) C. Zeng, P. L. Wu, Z. T. Dong, X. Li, Y. F. Zhou, Q. Xue, *Reproduction* **2020**, *160*, 481.
26. M. Rohrmoser, M. Hölzel, T. Grimm, A. Malamoussi, T. Harasim, M. Orban, I. Pfisterer, A. Gruber-Eber, E. Kremmer, D. Eick, *Mol. Cell. Biol.* **2007**, *27*, 3682.
27. L. Cheng, B. Yuan, S. Ying, C. Niu, H. Mai, X. Guan, X. Yang, Y. Teng, J. Lin, J. Huang, R. Jin, J. Wu, B. Liu, S. Chang, E. Wang, C. Zhang, N. Hou, X. Cheng, D. Xu, X. Yang, S. Gao, Q. Ye, *Sci. Adv.* **2019**, *5*, eaav1090.
28. Y. Sun, Q. Wang, M. Wang, F. Sun, P. Qiao, A. Jiang, C. Ren, Z. Yu, T. Yang, *Cell. Mol. Life Sci. CMLS* **2022**, *80*, 13.
29. D. Kalathil, S. John, A. S. Nair, *Front. Oncol.* **2020**, *10*, 626836.
30. D. Balli, Y. Zhang, J. Snyder, V. V. Kalinichenko, T. V. Kalin, *Cancer Res.* **2011**, *71*, 40.
31. M. A. Khan, J. Sengupta, L. C. Giudice, S. Mittal, S. Kumar, S. D. Gupta, R. Sharma, A. R. Najwa, D. Ghosh, *J. Endometr.* **2011**, *3*, 8.
32. D. Kopanja, V. Chand, E. O'Brien, N. K. Mukhopadhyay, M. P. Zappia, A. Islam, M. V. Frolov, B. J. Merrill, P. Raychaudhuri, *Cancer Res.* **2022**, *82*, 2458.
33. a) N. K. Mukhopadhyay, V. Chand, A. Pandey, D. Kopanja, J. R. Carr, Y. J. Chen, X. Liao, P. Raychaudhuri, *Sci. Rep.* **2017**, *7*, 46017; b) I. Wierstra, J. Alves, *Biol. Chem.* **2006**, *387*, 949.
34. a) D. A. Sanders, C. S. Ross-Innes, D. Beraldi, J. S. Carroll, S. Balasubramanian, *Genome Biol.* **2013**, *14*, R6; b) P. A. Madureira, R. Varshochi, D. Constantinidou, R. E. Francis, R. C. Coombes, K. M. Yao, E. W. Lam, *J. Biol. Chem.* **2006**, *281*, 25167.

How to cite this article: J. Zhu, P. Wu, R. Lu, C. Zeng, C. Peng, Y. Zhou, Q. Xue, *VIEW.* **2023**, 20230090. https://doi.org/10.1002/VIW.20230090